Desalination and Water Treatment
www.deswater.com

doi: 10.1080/19443994.2014.947784

55 (2015) 2856–2867
August

Taylor & Francis
Taylor & Francis Group

Assessment of the use of solar thermal collectors for desalination

P. Horta[a,*], G. Zaragoza[b], D.C. Alarcón-Padilla[b]

[a]*University of Évora—BES Chair in Renewable Energies, Casa Cordovil, 2º Andar, Rua Dom Augusto Eduardo Nunes, 7, 7000-651 Évora, Portugal, email: phorta@uevora.pt (P. Horta)*
[b]*CIEMAT-Plataforma Solar de Almería, Ctra. de Senés s/n, 04200 Tabernas, Almería, Spain*

Received 17 April 2014; Accepted 16 June 2014

ABSTRACT

The use of renewable energy in desalination is the only sustainable way to decrease the water deficit without aggravating the energy crisis. Solar desalination is usually presented as the most optimal solution for sustainable desalination since the water needs are usually larger in places with high solar radiation. Considering the potential use of desalination as means of producing water in small isolated communities, the focus of this study lies on the use of solar energy in thermal desalination systems of small–medium capacity and low maintenance requirements. Based on typical values for the thermal energy requirements of such systems and on characteristic performance parameters of commercially available low-temperature solar thermal technologies, different system layouts are assessed and optimal system dimensioning is studied, for different locations, in terms of estimated water production costs.

Keywords: Solar desalination; Energy efficiency; Solar thermal collectors

1. Introduction

The use of renewable energy in desalination is the only sustainable way to decrease the water deficit without aggravating the energy crisis. Solar desalination is usually presented as the most optimal solution for sustainable desalination since the water needs are usually larger in places with high solar radiation. In this work, the feasibility of using solar energy for thermal desalination is assessed by analyzing the combination of low-temperature solar collection technologies with existing thermal desalination systems.

The focus of this study is decentralized water production, so desalination systems of small–medium capacity and low maintenance such as membrane distillation and humidification–dehumidification are considered.

Whereas large-scale desalination units might be operated in a cogeneration basis, with heat provided from a cheap (or even free of charge) source (such is the case of the larger thermal-based desalination systems), small–medium size desalination units might be potentially placed in areas where heat sources come with a price. In such cases, and even if solar energy

*Corresponding author.

Presented at the Conference on Desalination for the Environment: Clean Water and Energy 11–15 May 2014, Limassol, Cyprus

does not come for free, it can be financially advantageous considering the system lifetime.

In this article, a simplified approach, based on thermal energy requirements and on characteristic solar collector performance parameters, enables an optimal system dimensioning from the perspective of water production costs. More than a detailed system behavior analysis, such approach enables a mapping of solar and desalination technologies whose combination, under a given system components cost and fuel price framework, stands for minimized water production costs.

Following this approach and objective, the article is organized as follows:

- In Section 2, the definitions of solar collector parameters for medium- and high-grade collectors, different desalination thermal requirements, and system layouts and operation parameters are presented.
- Within Section 3, system simulation results are presented, in terms of solar fraction (ratio between the energy delivered by the solar system and the total energy delivered to the desalination system), for two different system layouts (with or without thermal storage) and three different locations (Abu Dhabi, Almeria, and Cairo).
- In Section 4, a range of financial analysis parameters are defined, and results on solar-related water production costs and optimal system dimensioning are presented for the system layouts and locations considered.
- In Sections 5 and 6, an analysis of results and concluding remarks are presented.

Typical values of the thermal energy requirements for each desalination system, based on pilot plant assessment and projections, are used. According to their thermal needs, suitable solar fields are designed in each case for a reference value of the total water production.

Commercially available low-temperature solar thermal technologies are considered in the simulations. Given the multiplicity of technologies (flat-plate, compound parabolic concentrators (CPC), evacuated tube solar collectors (ETC)) and marketed solutions, higher and lower boundaries to solar field performance are defined.

Two configurations, with and without the presence of water-based thermal storage, are considered within this study. Considering year-round operation, both configurations make use of a backup heat production system. For each of the system configurations considered, solar fraction values are calculated for different solar field areas (and thermal storage volumes).

The results obtained are used as input data to a preliminary cost analysis in order to assess the solar-related costs of each configuration, allowing to compare the levelized water cost obtained. Such techno-economic analysis is extended to three different locations at different geographical latitudes (and climate conditions), enabling an assessment of the impact of solar collector characteristics, solar field (and thermal storage) dimensioning, and overall yearly performance in the (solar-related) water cost.

2. Framework definition

2.1. Solar field definition

Considering the focus of this study on decentralized, small-to-medium-capacity and low-maintenance water production systems, the solar field composition is based on stationary solar thermal collectors.

Stationary collectors rely on three basic technological concepts: flat-plate, CPC, and ETC. The development of the solar thermal collectors market in the last decade can be illustrated with the evolution of Solar Keymark licenses attributed from the beginning of this European certification scheme: from its first certificate, in 2003, more than 1,600 licenses were registered by 2013, from over 700 companies in 40 countries (27 European and 13 non-European) [1].

At present, stationary solar collector products are available following not only those basic technological concepts but also their combinations; for example, flat-plate evacuated collectors (FPC) or evacuated tube collectors with CPC concentrators. Regardless of their technological concept, solar collectors are optically and thermally characterized after a standardized methodology [2] based on a suitable collector model.

In this study, the steady-state efficiency test method is used, in view of its wider use (to the present). According to this method, the collector efficiency curve is described by three parameters (considering a glazed collector): the optical efficiency η_0, a global heat loss coefficient a_1, and a temperature-dependent coefficient for the global heat loss coefficient a_2.

The test includes also the measurement of incidence angle modifiers (IAM), $K(\theta)$, based on hemispherical irradiance, to be used in instantaneous power calculations. Again, it is not possible to assign a specific IAM curve to a specific technology. Yet, different technologies present optical specificities enabling the adoption of representative IAM curves for transversal incidence conditions, namely:

- FPC optical efficiency decreases continuously with increasing incidence angles due to increasing reflection on the flat glass cover.
- CPC optical efficiency presents abrupt reductions for incidences larger than truncation and acceptance angles (optical efficiency drops to zero).
- ETC might present increases in optical efficiency up to medium-range incidences due to absorber incidence conditions (e.g. flat absorber tubes) or to reduced number of reflections in back reflectors (for ETC with back reflector configurations).

For longitudinal incidence, a single glazing approximation ($b_0 = -0.1$) is assumed [3], following the overall IAM considered for FPCs. Under these assumptions, the IAM values chosen, in the present article, for FPC, CPC, and ETC models are in accordance with Table 1.

The calculation of instantaneous collector power from steady-state efficiency curve parameters follows Eq. (1):

$$\dot{Q}_{\mathrm{col}} = \eta_0 K(\theta) G_{\mathrm{col}} A_a - a_1 (T_f - T_a) A_a - a_2 (T_f - T_a)^2 A_a \tag{1}$$

Given the multiplicity of solar collectors available, both in terms of technological concepts and material quality options, it is difficult to point specific parameter values for each technology. The approach used in this study uses a range of values for each parameter, as follows:

- $0.55 \le \eta_0 \le 0.83$ (from a low-grade ETC to a high-grade FPC);
- $1.0 \le a_1 \le 5.0\,\mathrm{W/m^2\,K}$ (from high-grade ETC to a low-grade non-evacuated collector); and
- $0.005 \le a_2 \le 0.015\,\mathrm{W/m^2\,K^2}$ (high-grade ETC to a low-grade collector).

Two different collector cases are considered, representing an upper and lower boundary of solar field performance considering common marketed collector efficiency parameters:

- High-grade ETC (HG): $\eta_0 = 0.72$; $a_1 = 1.0\,\mathrm{W/m^2\,K}$; $a_2 = 0.005\,\mathrm{W/m^2\,K^2}$; ETC-like IAM.
- Medium-grade FPC (MG): $\eta_0 = 0.80$; $a_1 = 3.0\,\mathrm{W/m^2\,K}$; $a_2 = 0.015\,\mathrm{W/m^2\,K^2}$; FPC-like IAM.

The solar field is assumed to be positioned at a 0° azimuth (facing South in Northern Hemisphere locations and facing North in Southern Hemisphere locations) with a tilt angle, β = latitude—5°.

2.2. Desalination system definition

Thermal desalination systems are based on evaporation and condensation. Their thermal efficiency is related to the energy recovery from the condensation process, which is used to preheat the feed water or to drive additional evaporation processes.

This work focuses on solar thermal desalination for decentralized water production. Therefore, small–medium-capacity systems with low maintenance such as membrane distillation and humidification–dehumidification have been considered.

The temperature of the heat input to the selected desalination systems has been fixed at 80°C, which matches the operational conditions of these technologies and can be supplied with acceptable performance from static solar collectors. The desalination system is operated 8 h/d (working period centered at solar noon), in-line with the normal operation of small–medium-capacity systems.

The desalination technologies have been categorized in four cases according to the parameters presented in Table 2. Different values for the specific thermal energy consumption have been considered (see Table 2). In desalination, thermal efficiency is expressed using an energy ratio which relates the latent heat required to vaporize the total distillate produced to the rate of heat supplied to the system (usually called gain output ratio, GOR). Cases 1 and 2 correspond approximately to systems with GOR 1 and 2. This can represent technologies with low efficiency like very basic humidification–dehumidification systems [4] or plate and frame membrane distillation

Table 1
IAM values assumed for FPC, CPC, and ETC type

Incidence (°)	0	10	20	30	40	50	60	70	80	90
FPC, overall	1.00	1.00	0.99	0.98	0.97	0.94	0.90	0.81	0.52	0.00
CPC, transv	1.00	1.00	0.98	0.96	0.93	0.86	0.30	0.05	0.02	0.00
ETC, transv	1.00	1.03	1.05	1.10	1.20	1.15	1.05	0.80	0.50	0.00
CPC, ETC longit	1.00	1.00	0.99	0.98	0.97	0.94	0.90	0.81	0.52	0.00

Table 2
Desalination technology cases: specific heat consumption and heat inlet and outlet temperatures

Case	STEC [kWh/m^3]	Heat input T [°C]	Heat outlet T [°C]
1	600	80	70
2	300	80	70
3	150	80	70
4	75	80	70

modules [5] with minimum latent heat recovery. Cases 3 and 4 correspond to high-efficiency systems with GOR values approximately 4 and 8, respectively. These fall in the upper limit of spiral-wound air-gap membrane distillation [6] or multiple-effect humidification–dehumidification systems [7].

2.3. System layout and operation parameters

Year-round operation of the water production system implies the use of a backup heat source assuring the system operation even under low (or none) solar resource conditions. Aiming an increased solar-based operation, the use of thermal energy storage (TES) is considered. In order to perform an analysis of the economic benefits of using a TES system, a solar + backup (no TES) layout is also simulated (Fig. 1).

System simulations are performed for different solar field characteristics, TES volumes, and system locations according to the following operation parameters:

- the desalination system operates at fixed $T_{heat,in}$ and $T_{heat,out}$, according to a fixed specific heat consumption;
- $T_{solar,in} = T_{stor}$ (w/TES) or $T_{solar,in} = T_{heat,out} +$ DHX (w/out TES);
- a fixed temperature differential DHX = 5°C is assumed at the heat exchanger;
- heat is extracted from the thermal storage only when $T_{stor} \leq T_{heat,out} +$ DHX;
- the backup system provides the temperature differential ($T_{heat,in}$ + DHX—$T_{back,in}$), with $T_{back,in} =$ max(T_{stor}, $T_{heat,out}$ + DHX) or $T_{back,in} =$ max(T_{solar}, $T_{heat,out}$ + DHX), that is, priority is given to the solar field (or solar fed TES);
- the thermal storage has a maximum temperature $T_{stor,max} = 95$°C, above which no heat input from the solar field is admitted (heat is rejected);
- the desalination unit works continuously at a fixed production rate within a daily production period of 8 h centered at solar noon; and
- circuit and storage heat losses are neglected.

3. Simulation results

System yearly operation simulations were performed with the two solar collector cases and for each of the desalination technologies and system layouts, in three different locations: Almeria (SP), Cairo (EGY), and Abu Dhabi (UAE). The system is simulated (and dimensioned) for a specific distillate production of 1 m^3/d.

System operation results are presented in terms of solar fraction, that is, the fraction of heat supplied to the desalination system (to produce 1 m^3/d) being supplied by the solar field (directly or via TES, depending on the system configuration).

3.1. System w/TES

As an example of the calculations performed, solar fraction values obtained for desalination systems 1 and 4 with MG and HG collectors, for Cairo, are presented in Fig. 2.

As means of comparing the results obtained for the different desalination cases and locations, results for the solar field dimensioning are presented, in

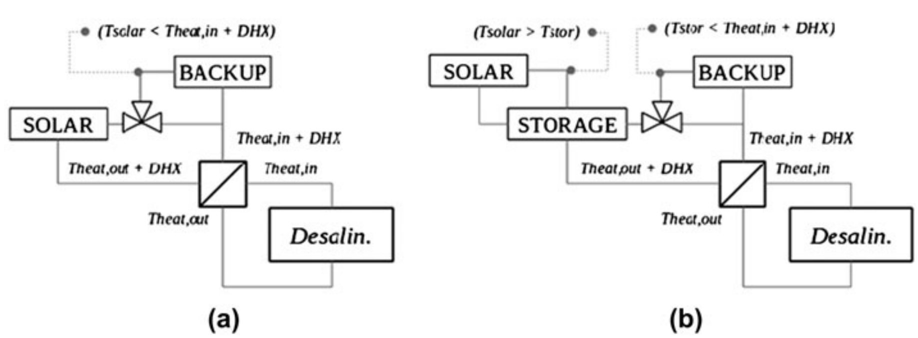

Fig. 1. System layouts: (a) solar + backup and (b) solar + TES + backup.

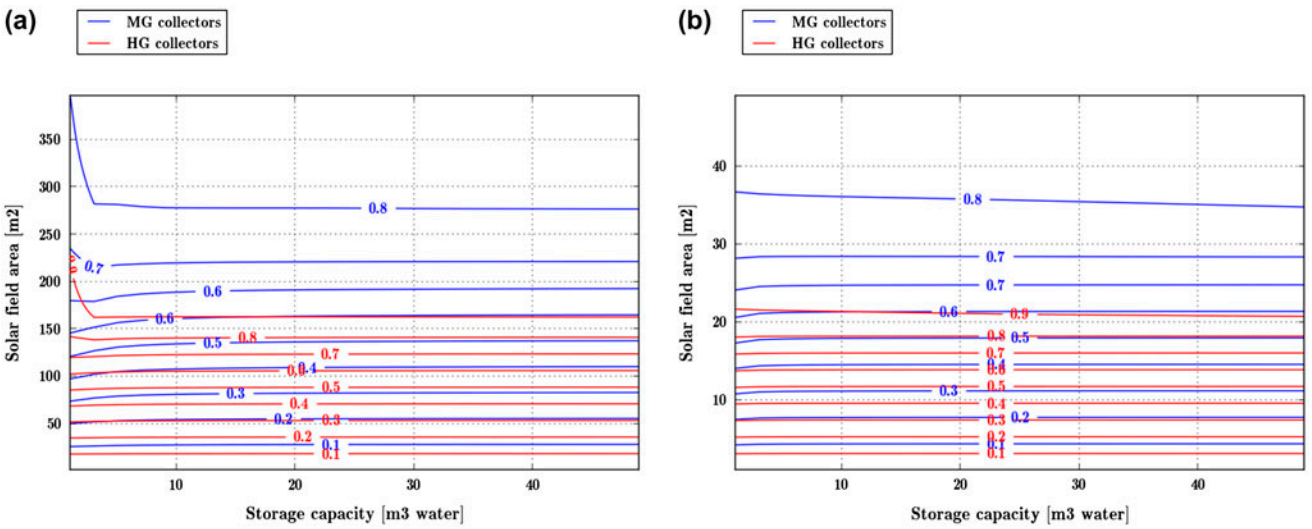

Fig. 2. Solar fraction results for Cairo, with a solar field composed of HG collectors or MG collectors for desalination systems: (a) 1 (600 kWh/m^3) and (b) 4 (75 kWh/m^3).

Table 3, fixing a solar fraction of 50% with a TES volume of 21 m^3. Such results illustrate the calculations performed for each system and location (over a much wider range of solar fractions and TES volumes), fully embedded in the results presented henceforth, for water production costs.

3.2. System w/out TES

As an example of the calculations performed, solar fraction values obtained for desalination systems 1 and 4 with MG and HG collectors, for Cairo, are presented in Fig. 3.

The results presented in Table 4, for the system dimensioning reaching a solar fraction of 50%, summarize the simulations performed for different solar collectors and desalination systems in Abu Dhabi (UAE), Almeria (SP), and Cairo (EGY), respectively.

4. Water cost analysis

An assessment of the water costs obtained for the different cases is based on a range of costs for the solar field and for the backup system fuel price. For this analysis, the following assumptions are taken:

- thermal storage price is linearly dependent on the storage volume, with a cost of 100 €/m^3 [8];
- backup heat production costs in the range 0.05–0.25 €/kWh;
- solar field costs in the range 50–300 €/m^2;
- minimum water costs correspond to the optimized dimensioning of the system, which takes into account an economic optimization of the system considering the solar fraction, the solar-related investment, and the fuel price; and
- the system has a lifetime of 20 years.

Table 3
Solar field dimensioning for a 50% solar fraction with a 21 m^3 TES in Abu Dhabi (UAE), Almeria (SP), and Cairo (EGY)

		Solar field area [m^2]		
Solar collector	Desalination system	Abu Dhabi	Almeria	Cairo
HG	1 (600 kWh/m^3)	89.6	103.5	88.3
	2 (300 kWh/m^3)	44.9	51.9	44.2
	3 (150 kWh/m^3)	22.5	26.0	22.1
	4 (75 kWh/m^3)	12.0	14.1	11.8
MG	1 (600 kWh/m^3)	141.7	192.8	148.7
	2 (300 kWh/m^3)	71.3	97.2	74.9
	3 (150 kWh/m^3)	35.8	48.6	37.6
	4 (75 kWh/m^3)	18.2	24.5	19.2

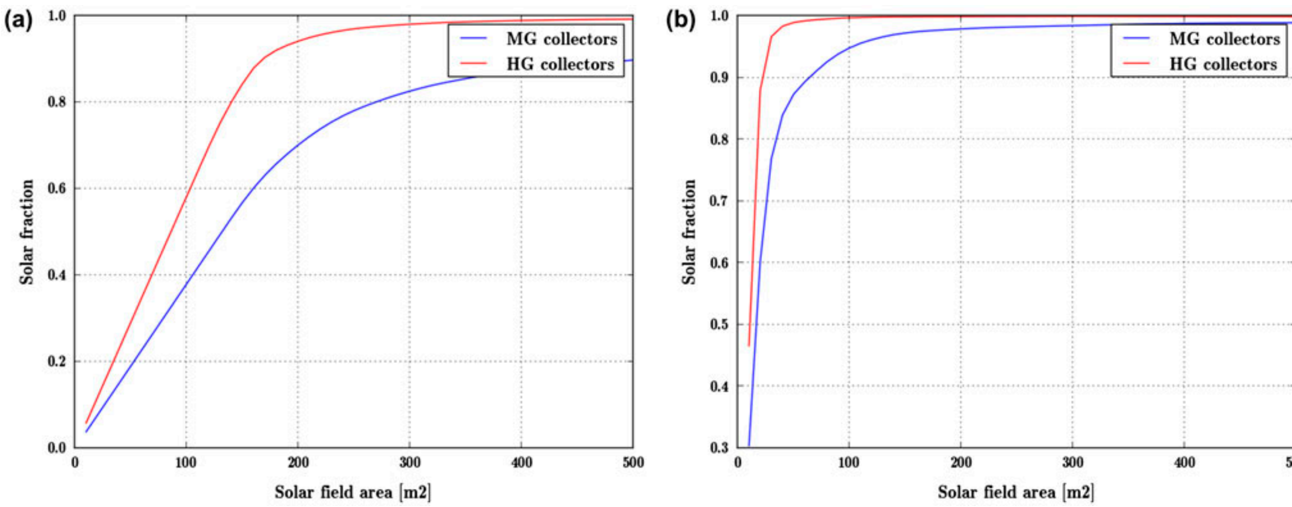

Fig. 3. Solar fraction results for Cairo, with a solar field composed of HG collectors or MG collectors for desalination systems: (a) 1 (600 kWh/m^3) and (b) 4 (75 kWh/m^3).

Table 4
Solar field dimensioning for a 50% solar fraction in Abu Dhabi (UAE), Almeria (SP), and Cairo (EGY)

		Solar field area [m^2]		
Solar collector	Desalination system	Abu Dhabi	Almeria	Cairo
HG	1 (600 kWh/m^3)	87.6	100.3	85.9
	2 (300 kWh/m^3)	43.8	50.1	42.9
	3 (150 kWh/m^3)	21.9	25.1	21.5
	4 (75 kWh/m^3)	11.1	13.0	10.8
MG	1 (600 kWh/m^3)	126.6	174.9	131.5
	2 (300 kWh/m^3)	63.3	87.6	65.8
	3 (150 kWh/m^3)	31.8	44.1	33.0
	4 (75 kWh/m^3)	16.0	22.4	16.6

Water costs are presented, for the optimized system dimensioning, according to four different perspectives:

- Solar system-related costs (SSC): specific water cost comprising only the solar field (and TES system) costs.
- Solar operation-related costs (SOC): specific water cost comprising the solar field (and TES system) costs and the backup fuel costs (excluding the backup system cost).
- Fuel-based operation costs (FBC): specific water cost for a fuel-based operation.
- Difference to backup-based operation (DBC): difference in specific water cost for a fuel-based operation (DBC = SOC—FBC), that is, this value can be regarded as a net benefit (when DBC < 0) of the solar system investment (not including an actualization rate).

Backup and desalination system costs (investment and maintenance) are not included in the analysis, which seeks to estimate the share of the water production cost due to the solar system. Following these assumptions, water production costs vs. system dimensioning results are presented.

4.1. System w/TES

As an example of the calculations performed, optimized solar operation-related (SOC) water costs and system dimensioning results obtained with MG and HG collectors in Abu Dhabi, for desalination systems 1 and 4, are presented in Figs. 4 and 5, respectively. In the graphics, different cost lines are presented for different solar field/fuel prices combinations. For a given solar field/fuel price combination, a water cost follows

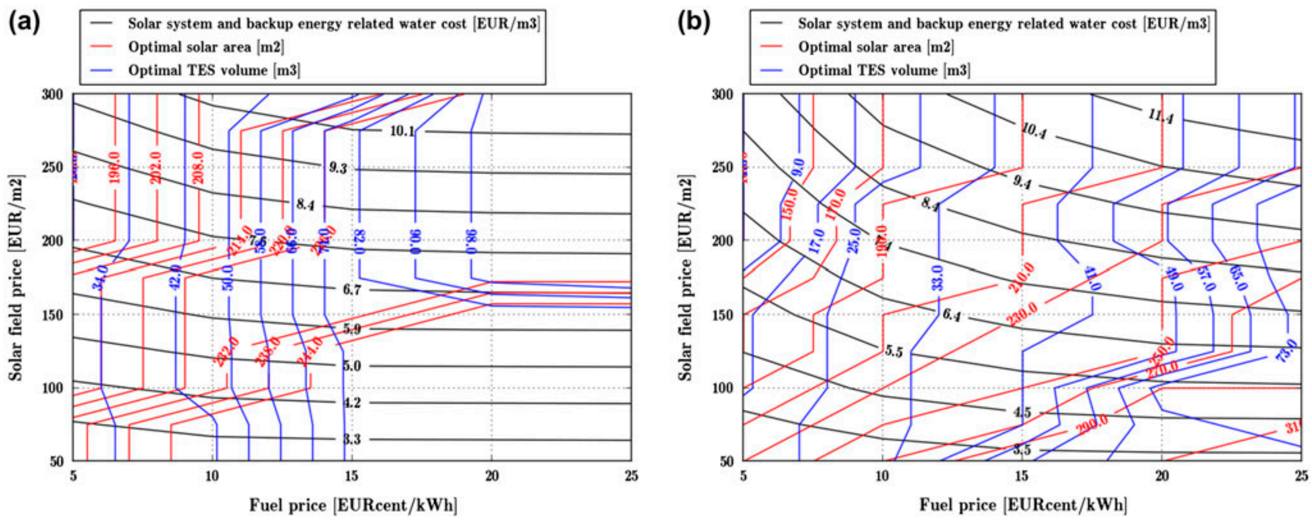

Fig. 4. Optimized solar operation related (SOC) water costs and system dimensioning for desalination system 1 (600 kWh/m^3), in Abu Dhabi (UAE), with a solar field composed of (a) HG collectors or (b) MG collectors.

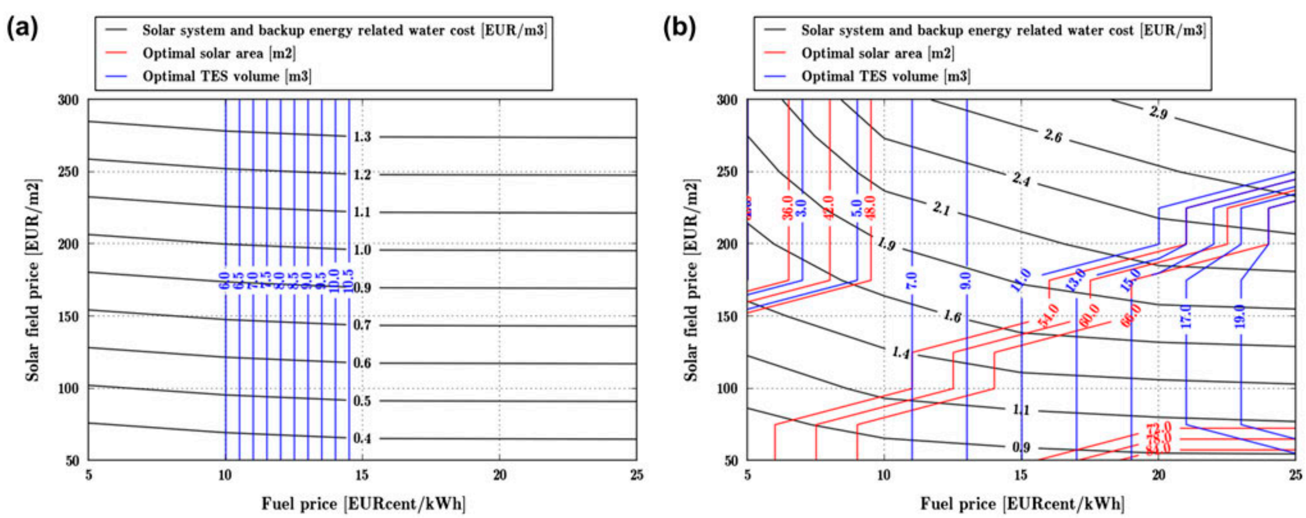

Fig. 5. Optimized solar operation related (SOC) water costs and system dimensioning for desalination system 4 (75 kWh/m^3), in Abu Dhabi (UAE), with a solar field composed of (a) HG collectors (result stands for a 30 m^3 solar field) or (b) MG collectors.

from the optimized system dimensioning presented, in the graphic, for the same point.

The results presented in Tables 5–7 summarize the results obtained for water costs, and corresponding optimal system dimensioning, considering a backup heat production price of 0.10 €/kWh and a solar field cost of 150 €/m^2, in Abu Dhabi (UAE), Almeria (SP), and Cairo (EGY), respectively.

4.2. System w/out TES

As an example of the calculations performed, optimized solar operation related (SOC) water costs and system dimensioning results obtained with MG and HG collectors in Abu Dhabi, for desalination systems 1 and 4, are presented in Figs. 6 and 7, respectively.

The results presented in Tables 8–10 summarize the results obtained for the minimum solar related

Table 5
Specific water costs for optimal system dimensioning in Abu Dhabi (UAE), considering a backup heat production price of 0.10 €/kWh, a TES cost of 100 €/m^3, and a solar field cost of 150 €/m^2

Solar collector	Desalination system	SSC [€/m^3]	SOC [€/m^3]	DBC [€/m^3]	Optimal solar field [m^2/m^3dist]	Optimal storage volume [m^3/m^3dist]	Solar fraction
HG	1 (600 kWh/m^3)	5.36	5.94	−54.06	230.0	46.0	0.99
	2 (300 kWh/m^3)	2.62	2.95	−27.05	110.0	26.0	0.99
	3 (150 kWh/m^3)	1.18	1.59	−13.41	50.0	11.0	0.97
	4 (75 kWh/m^3)	0.70	0.75	−6.75	30.0	6.0	0.99
MG	1 (600 kWh/m^3)	9.26	12.24	−47.76	410.0	61.0	0.95
	2 (300 kWh/m^3)	4.74	6.13	−23.87	210.0	31.0	0.95
	3 (150 kWh/m^3)	2.48	3.09	−11.91	110.0	16.0	0.96
	4 (75 kWh/m^3)	1.11	1.54	−5.96	50.0	6.0	0.94

Table 6
Specific water costs for optimal system dimensioning in Almeria (SP), considering a backup heat production price of 0.10 €/kWh, a TES cost of 100 €/m^3, and a solar field cost of 150 €/m^2

Solar collector	Desalination system	SSC [€/m^3]	SOC [€/m^3]	DBC [€/m^3]	Optimal solar field [m^2/m^3dist]	Optimal storage volume [m^3/m^3dist]	Solar fraction
HG	1 (600 kWh/m^3)	7.82	8.65	−51.35	310.0	106.0	0.99
	2 (300 kWh/m^3)	3.78	4.32	−25.68	150.0	51.0	0.98
	3 (150 kWh/m^3)	1.73	2.17	−12.83	70.0	21.0	0.97
	4 (75 kWh/m^3)	1.18	1.19	−6.31	50.0	11.0	1.00
MG	1 (600 kWh/m^3)	13.85	19.77	−40.23	590.0	126.0	0.90
	2 (300 kWh/m^3)	6.79	9.89	−20.11	290.0	61.0	0.90
	3 (150 kWh/m^3)	3.51	4.94	−10.06	150.0	31.0	0.90
	4 (75 kWh/m^3)	1.66	2.48	−5.02	70.0	16.0	0.89

Table 7
Specific water costs for optimal system dimensioning in Cairo (EGY), considering a backup heat production price of 0.10 €/kWh, a TES cost of 100 €/m^3, and a solar field cost of 150 €/m^2

Solar collector	Desalination system	SSC [€/m^3]	SOC [€/m^3]	DBC [€/m^3]	Optimal solar field [m^2/m^3dist]	Optimal storage volume [m^3/m^3dist]	Solar fraction
HG	1 (600 kWh/m^3)	5.15	6.28	−53.72	230.0	31.0	0.98
	2 (300 kWh/m^3)	2.41	3.16	−26.84	110.0	11.0	0.98
	3 (150 kWh/m^3)	1.11	1.69	−13.31	50.0	6.0	0.96
	4 (75 kWh/m^3)	0.70	0.79	−6.71	30.0	6.0	0.99
MG	1 (600 kWh/m^3)	9.67	13.51	−46.49	450.0	31.0	0.94
	2 (300 kWh/m^3)	4.95	6.76	−23.24	230.0	16.0	0.94
	3 (150 kWh/m^3)	2.34	3.38	−11.62	110.0	6.0	0.93
	4 (75 kWh/m^3)	1.11	1.73	−5.77	50.0	6.0	0.92

water costs, and corresponding optimal system dimensioning, considering a backup heat production price of 0.10 €/kWh, in Abu Dhabi (UAE), Almeria (SP), and Cairo (EGY), respectively.

5. Discussion of results

From the results obtained, it is straightforward to highlight that when energy has a cost, producing water inefficiently stands for prohibitive water costs, regardless of the heat production option taken: solar-driven or fuel-driven.

Departing from this conclusion, the results obtained in the simulations conducted for the different system layouts show that:

- the costs associated with the solar energy supply are highly dependent on the specific thermal

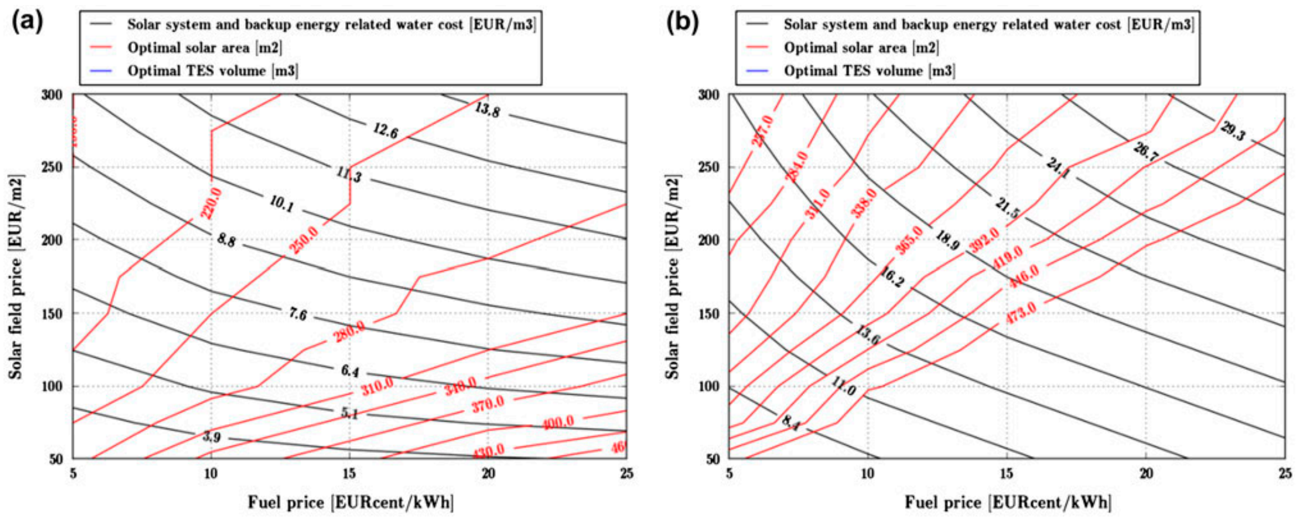

Fig. 6. Optimized solar operation related (SOC) water costs and system dimensioning for desalination system 1 (600 kWh/m^3), in Abu Dhabi (UAE), with a solar field composed of (a) HG collectors or (b) MG collectors.

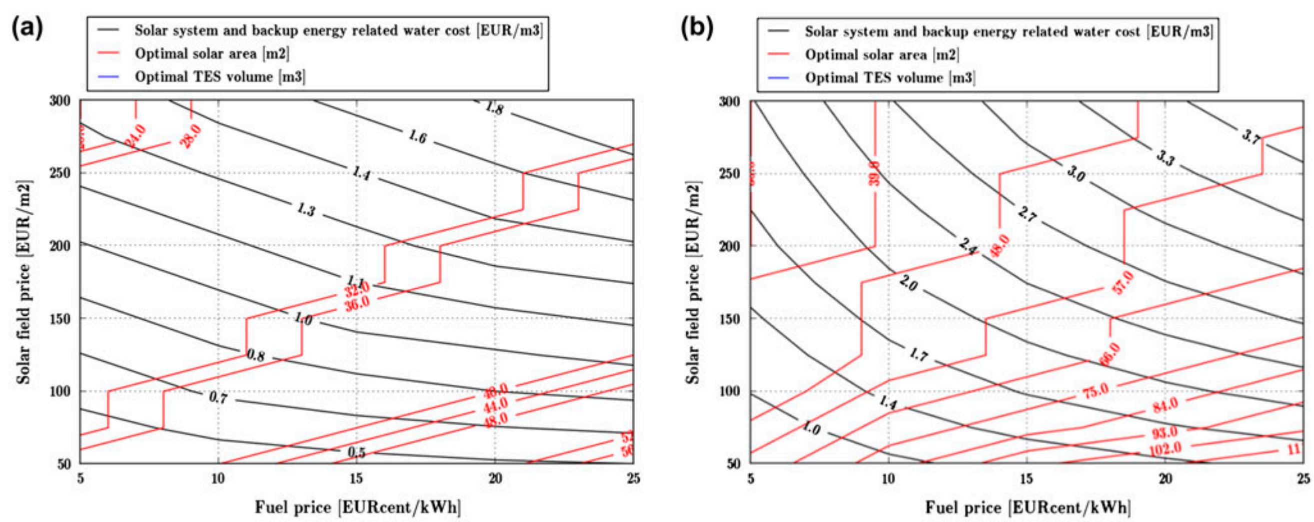

Fig. 7. Optimized solar operation related (SOC) water costs and system dimensioning for desalination system 4 (75 kWh/m^3), in Abu Dhabi (UAE), with a solar field composed of (a) HG collectors or (b) MG collectors.

energy consumption of the desalination system. Only for the highest values of the thermal efficiency considered, the solar-related costs are below 2 €/m^3;

- these values of thermal efficiency, however, are at the grasp of current thermal desalination technologies which can be applied for small–medium-capacity stand-alone applications like the one considered here; as a matter of fact, the values of case 3 (GOR approximately 4) are close to what can be reached with state-of-the-art membrane distillation [9] and humidification–dehumidification [10], while current projections for these technologies fall in case 4 (GOR approximately 8);
- even if solar collector costs follow collector performance, it is important to acknowledge that in face of the operating temperatures in stake (both in TES and in the desalination system), lower solar-related costs might be achieved using higher performance collectors (as reflected on reductions of water production cost in the order

Table 8
Specific water costs for optimal system dimensioning in Abu Dhabi (UAE), considering a backup heat production price of 0.10 €/kWh and a solar field cost of 150 €/m^2

Solar collector	Desalination system	SSC [€/m^3]	SOC [€/m^3]	DBC [€/m^3]	Optimal solar field [m^2/m^{3}dist]	Solar fraction
HG	1 (600 kWh/m^3)	5.14	7.08	−52.92	250.0	0.97
	2 (300 kWh/m^3)	2.67	3.55	−26.45	130.0	0.97
	3 (150 kWh/m^3)	1.23	1.78	−13.22	60.0	0.96
	4 (75 kWh/m^3)	0.62	0.89	−6.61	30.0	0.96
MG	1 (600 kWh/m^3)	7.81	14.41	−45.59	380.0	0.89
	2 (300 kWh/m^3)	3.90	7.20	−22.80	190.0	0.89
	3 (150 kWh/m^3)	1.85	3.61	−11.39	90.0	0.88
	4 (75 kWh/m^3)	1.03	1.81	−5.69	50.0	0.90

Table 9
Specific water costs for optimal system dimensioning in Almeria (SP), considering a backup heat production price of 0.10 €/kWh and a solar field cost of 150 €/m^2

Solar collector	Desalination system	SSC [€/m^3]	SOC [€/m^3]	DBC [€/m^3]	Optimal solar field [m^2/m^{3}dist]	Solar fraction
HG	1 (600 kWh/m^3)	7.81	11.75	−48.25	380.0	0.93
	2 (300 kWh/m^3)	3.90	5.88	−24.12	190.0	0.93
	3 (150 kWh/m^3)	1.85	2.94	−12.06	90.0	0.93
	4 (75 kWh/m^3)	1.03	1.47	−6.03	50.0	0.94
MG	1 (600 kWh/m^3)	8.84	25.51	−34.49	430.0	0.72
	2 (300 kWh/m^3)	4.32	12.76	−17.24	210.0	0.72
	3 (150 kWh/m^3)	2.26	6.38	−8.62	110.0	0.73
	4 (75 kWh/m^3)	1.03	3.19	−4.31	50.0	0.71

Table 10
Specific water costs for optimal system dimensioning in Cairo (EGY), considering a backup heat production price of 0.10 €/kWh and a solar field cost of 150 €/m^2

Solar collector	Desalination system	SSC [€/m^3]	SOC [€/m^3]	DBC [€/m^3]	Optimal solar field [m^2/m^{3}dist]	Solar fraction
HG	1 (600 kWh/m^3)	5.14	6.94	−53.06	250.0	0.97
	2 (300 kWh/m^3)	2.47	3.48	−26.52	120.0	0.97
	3 (150 kWh/m^3)	1.23	1.74	−13.26	60.0	0.97
	4 (75 kWh/m^3)	0.62	0.87	−6.63	30.0	0.97
MG	1 (600 kWh/m^3)	7.81	15.77	−44.23	380.0	0.87
	2 (300 kWh/m^3)	3.90	7.89	−22.11	190.0	0.87
	3 (150 kWh/m^3)	2.05	3.96	−11.04	100.0	0.87
	4 (75 kWh/m^3)	1.03	1.98	−5.52	50.0	0.87

of 50%, when considering a high-grade over a medium-grade solar collector);

- the use of TES stands for a cost reduction highly dependent on its cost (100 €/m^3 used from a range 50–200 €/m^3). For the financial constrains presented in the tables (solar field costs of 150 €/m^2 and TES costs of 100 €/m^3), the cost reduction of using TES is less significant; and
- the interest on using TES depends highly on the collector performance under the operation temperature conditions (in between 70 and 95°C, for the presented cases).

6. Conclusions

Whereas large-scale desalination units might be operated in a cogeneration basis, with heat provided from a cheap (or even free of charge) source (such is the case of the larger thermal-based desalination systems), small–medium size desalination units might be potentially placed in areas where heat sources come with a price. In such cases, and even if solar energy does not come for free, it can be financially advantageous, considering the system lifetime.

In this article, a simplified approach, based on thermal energy requirements and on characteristic solar collector performance parameters, enables a mapping of solar and desalination technologies whose combination, under a given system components cost and fuel price framework, stands for minimized water production costs.

The results show that, on one side, less efficient desalination systems presenting higher thermal requirements need larger solar fields and thus are penalized with higher solar-related water production costs. However, when energy comes with a price, higher energy requirements might be met with a solar-driven system in a less expensive way, depending on the price of the available conventional energy source.

Yet, regarding minimized water production costs, it is clear that higher efficiency desalination systems are required, especially when efficiency increases are followed by technology cost increases at a lower rate, the same applying to the choice of solar collector technologies.

The use of energy storage has a lesser influence in the costs, which of course is highly dependent on the cost of the TES systems.

The basic approach presented tries to set boundary conditions for the interest and viability of solar thermal-driven desalination, influenced both by the thermal efficiency parameters of the system components and by their price, under a specific framework of solar radiation conditions and available conventional energy sources price. The analysis of a specific combination of technologies requires a more thorough approach, including:

- thermal losses in the circuits and storage system;
- an optimization of system operation in terms of solar field, thermal storage, and desalination heat input temperatures; and
- an optimization of system operation in terms of desalination system operation periods, which might be adapted to the energy availability, allowing for a non-stationary performance (different to the operation at constant energy supply which has been contemplated in this paper), in which case the storage of water to regulate the demand can be introduced as an alternative to the provision of a larger solar thermal field or the storage of energy to adapt to the solar variability.

Nomenclature

A_a	—	collector aperture area (m^2)
a_2	—	global heat loss coefficient ($W/m^2 K$)
a_2	—	temperature-dependent heat loss coefficient ($W/m^2 K^2$)
G_{col}	—	global irradiance incident on the collector aperture plane (W/m^2)
η_0	—	collector optical efficiency
$K(\theta)$	—	beam radiation IAM (steady-state test)
T_a	—	air temperature (℃)
T_f	—	average heat transfer fluid temperature (℃)
β	—	tilt angle (°)
$T_{back,in}$	—	backup system input heat temperature (℃)
$T_{solar,in}$	—	solar field input heat temperature (℃)
T_{stor}	—	thermal storage temperature (℃)
$T_{heat,in}$	—	desalination system input heat temperature (℃)
$T_{heat,out}$	—	desalination system output heat temperature (℃)
DHX	—	heat exchanger temperature differential (hot to cold side) (℃)
STEC	—	specific thermal energy consumption (kWh/m^3)

References

[1] Available from: http://www.estif.org/solarkeymarknew/index.php (in February 2014).

[2] ISO 9806:2013, Solar energy—Solar thermal collectors—Test methods. Available from: http://www.iso.org/iso/home.htm.

[3] A.F. Souka, H.H. Safwat, Determination of the optimum orientations for the double-exposure, flat-plate collector and its reflectors, Sol. Energy 10(4) (1966) 170–174.

[4] G.P. Narayan, M.H. Sharqawy, E.K. Summers, J.H. Lienhard, S.M. Zubair, M.A. Antar, The potential of solar-driven humidification–dehumidification desalination for small-scale decentralized water production, Renew. Sust. Energy Rev. 14 (2010) 1187–1201.

[5] E. Guillén-Burrieza, G. Zaragoza, S. Miralles-Cuevas, J. Blanco, Experimental evaluation of two pilot-scale membrane distillation modules used for solar desalination, J. Membr. Sci. 409–410 (2012) 264–275.

[6] G. Zaragoza, A. Ruiz-Aguirre, E. Guillén-Burrieza, Efficiency in the use of solar thermal energy of small membrane desalination systems for decentralized water production, Appl. Energy (2014), doi: 10.1016/j.apenergy.2014.02.024.

[7] H. Müller-Holst, M. Engelhardt, M. Herve, W. Schölkopf, Solar thermal seawater desalination systems for decentralised use, Renew. Energy 14(1–4) (1998) 311–318.
[8] Thermal Energy Storage—Technology Brief, IEA-ETSAP and IRENA Technology Brief E17—January 2013. Available from: www.irena.org/Publications.
[9] A. Ruiz-Aguirre, D.C. Alarcón-Padilla, G. Zaragoza, Productivity analysis of two spiral-wound membrane distillation prototypes coupled with solar energy, in: Proceedings of the European Desalination Society Conference on Desalination for the Environment, Clean Water and Energy, Limassol, Cyprus, May 2014.
[10] G. Prakash Narayan, M.G. St. John, S.M. Zubair, J.H. Lienhard, Thermal design of the humidification dehumidification desalination system: An experimental investigation, Int. J. Heat Mass Transfer 58 (2013) 740–748.